Articles

Physical Society of Indonesia

Journal of the Physical Society of Indonesia **2(1)**, 1-11 (2026)

https://doi.org/10.2566/10.35895/jpsi.2.1.1-11.2026

Co-Seismic Surface Deformation Associated with the 2 May 2025 Padang Panjang Earthquake Derived from Sentinel-1 DInSAR

Khairunnisa Khairunnisa[1*], Suaidi Ahadi[2], and Lori Agung Satria[3]

[1] *Department of Physics, Universitas Andalas, Padang, 25163, Indonesia*
[2] *Agency of Meteorology, Climatology, and Geophysics, Padang Panjang, 27118, Indonesia*

(Received November 06, 2025; revised February 09, 2026; accepted February 12, 2026; published online April 18, 2026)

This study analyzed surface deformation associated with the Mw 4.8 earthquake that occurred in Padang Panjang, West Sumatra, on May 2, 2025. The purpose of this research was to identify surface changes using Differential Interferometric Synthetic Aperture Radar (DInSAR) with Sentinel-1A imagery from the European Space Agency. The analysis covered the pre-earthquake period (April 8–May 2, 2025) and the post-earthquake period (May 2–June 7, 2025). The deformation values represented displacement along the satellite Line of Sight (LOS). The results showed a clear spatial change between the two periods. Before the earthquake, the area near the epicenter exhibited LOS displacement values of approximately +0.45 mm, while after the earthquake, the values decreased to around −0.045 mm, indicating relative subsidence along the LOS direction. The observed LOS displacement difference of about −0.495 mm suggested a surface response to seismic activity. However, the deformation magnitude was relatively small and may have been influenced by atmospheric effects, decorrelation, and interferometric noise. Therefore, the results were interpreted cautiously without strong tectonic attribution. This study demonstrated the capability of DInSAR to detect subtle surface deformation in seismic regions.

Keywords: *DInSAR, Earthquake, Padang Panjang, Sentinel-1A, Sianok Fault, Surface Deformation*

1. INTRODUCTION

Indonesia is located at the convergence of three major tectonic plates—the Indo-Australian, Eurasian, and Pacific plates—making it one of the most seismically active regions in the world (Pustlitbang PUPR, 2017). The continuous interaction of these plates results in the accumulation of tectonic stress that is periodically released as seismic energy, producing frequent earthquakes that are predominantly tectonic in origin (Rafie et al., 2023; Turcotte and Gerald, 2014). Such seismic events can induce ground surface deformation, including uplift and subsidence, which may affect land stability and infrastructure even when earthquakes are of moderate magnitude (Massonnet & Feigl, 1998).

West Sumatra Province is among the most earthquake-prone regions in Indonesia due to the presence of active fault systems, particularly the Sumatran Fault that extends along the Bukit Barisan Mountains and acts as a major crustal deformation zone (Rafie et al., 2023). One of its active segments, the Sianok Fault, frequently generates shallow local earthquakes. Seismotectonic studies indicate high seismic potential in this region, as reflected by relatively high a-values and low b-values in West Sumatra, suggesting intense seismic activity and stress accumulation (Raharjo et al., 2016).

On 2 May 2025, a Mw 4.8 earthquake occurred in Padang Panjang at a depth of approximately 10 km and was associated with the Sianok Fault segment (Sari, 2025). The earthquake caused minor damage and was felt at an intensity of III–IV MMI near the epicenter. Although classified as a moderate earthquake, events of this magnitude are scientifically important because they may generate subtle surface deformation that is difficult to detect using conventional field-based observations alone (Hanssen, 2001). Investigating such deformation is essential for improving the understanding of fault behavior and local seismic responses in densely populated areas.

*Contact Author: kkhairunnisa150@gmail.com

Direct field monitoring of surface deformation in tectonically active regions is often constrained by limited accessibility, safety considerations, and restricted spatial coverage. Consequently, satellite-based remote sensing provides an effective alternative for regional-scale monitoring. Remote sensing enables the acquisition of surface information without direct contact by detecting reflected or emitted electromagnetic energy (Jensen, 2015), making it particularly suitable for observing geophysical processes over wide and inaccessible areas.

Interferometric Synthetic Aperture Radar (InSAR) has been widely applied to detect ground surface deformation with millimeter-scale precision through phase difference analysis of radar signals acquired at different times (Massonnet & Feigl, 1998; Jensen, 2015). The C-band radar system onboard Sentinel-1 offers an optimal balance between surface sensitivity and vegetation penetration, making it suitable for moderately vegetated regions such as West Sumatra (Fajriani et al., 2019). InSAR measurements rely on signal coherence to detect changes in the satellite-to-ground distance, while the resulting interferogram contains contributions from topography, deformation, atmospheric delay, and orbital errors (Raimadoya et al., 2004; Hanssen, 2001). InSAR measurements rely on signal coherence to detect changes in the satellite-to-ground distance, while the resulting interferogram contains contributions from topography, deformation, atmospheric delay, and orbital errors (Pepe and Calò, 2017).

Differential InSAR (DInSAR) further refines this technique by removing the topographic phase component, allowing isolation of surface displacement signals related to geophysical processes (Pepe, 2012). DInSAR has been successfully applied to various seismic events in Indonesia, including the 2018 Lombok earthquake (Azhari et al., 2020), and the 2023 Sumedang earthquake, where deformation associated with the Cipeles Fault was identified (Oktaviani and Sari, 2024).

Despite these advances, the application of DInSAR to moderate-magnitude earthquakes in West Sumatra remains limited. Previous studies have mainly focused on large seismic events, leaving a research gap in understanding surface deformation related to smaller but frequent earthquakes. The availability of high-resolution Sentinel-1 imagery and accessible processing tools provides an opportunity to address this gap and demonstrate the methodological capability of DInSAR in such contexts (Palano, 2023).

Therefore, this study aimed to apply the DInSAR technique using Sentinel-1 imagery to identify and analyze surface deformation associated with the Mw 4.8 earthquake that occurred on 2 May 2025 in Padang Panjang. The objective of this research was to characterize the spatial pattern of coseismic surface displacement and to evaluate the capability of DInSAR in detecting subtle surface responses related to moderate seismic events in an active fault zone**.**

2. METHOD

2.1 Data

This study utilized Sentinel-1A Synthetic Aperture Radar (SAR) Single Look Complex (SLC) imagery to analyze co-seismic surface deformation associated with the earthquake that occurred on 2 May 2025 near Padang Panjang, West Sumatra. The epicenter was located approximately 2 km northeast of Padang Panjang at coordinates 0.45° LS and 100.41° BT, with a magnitude of Mw 4.8 and a focal depth of 10 km, as reported by the Meteorological, Climatological, and Geophysical Agency (BMKG). The earthquake occurred at 14:07:44 WIB and produced ground shaking with instrumental intensities ranging from II to VII, affecting surrounding areas, as illustrated in Figure 1.

The primary dataset consists of Sentinel-1A Synthetic Aperture Radar (SAR) images in Single Look Complex (SLC) format, acquired on three different dates:

- April 8, 2025 (Pre-earthquake)
- May 2, 2025 (Co-seismic)
- June 7, 2025 (Post-earthquake)

All images were acquired in Interferometric Wide (IW) swath mode with VV polarization and ascending orbit geometry. The use of a consistent orbit direction and acquisition geometry was intended to minimize geometric decorrelation and to maintain stable interferometric coherence. Given the relatively short temporal baselines (24 days and 36 days) and moderate land cover conditions in the

study area, a moderate-to-high coherence level was expected, particularly in urban and sparsely vegetated zones.

Descending orbit data were not included in this study due to limited temporal pairing consistency around the earthquake date and increased geometric decorrelation caused by different viewing geometries. Using only ascending orbit data ensured uniform Line-of-Sight (LOS) sensitivity and reduced uncertainty when comparing deformation patterns between pre- and post-earthquake periods.

Additional geospatial datasets included the Shuttle Radar Topography Mission (SRTM) Digital Elevation Model (DEM) with 30 m resolution for topographic phase removal and administrative boundary maps of Padang Panjang for visualization. All SAR data were obtained from the Copernicus Open Access Hub, while ancillary datasets were sourced from national geospatial data portals, as summarized in Table 1.

Atmospheric artifacts were considered a potential source of error, particularly because the expected deformation magnitude was on the millimeter scale. Although no explicit atmospheric correction model was applied, the use of short temporal baselines and comparison between pre- and post-event interferograms helped reduce long-wavelength atmospheric phase delays.

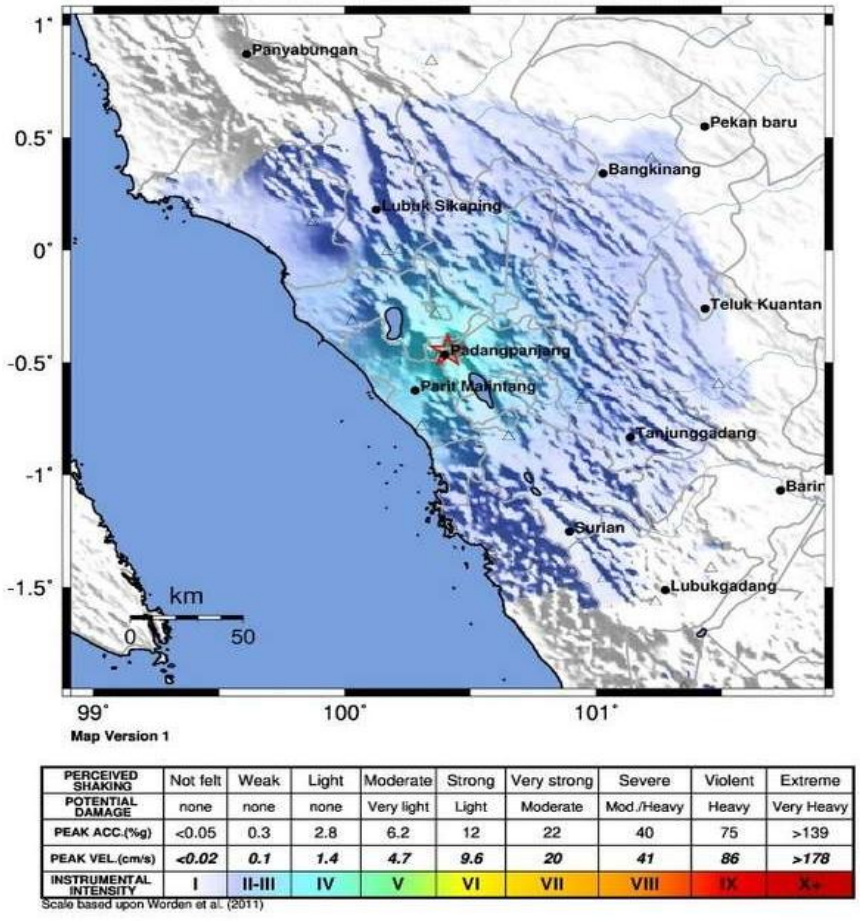

Figure 1. BMKG ShakeMap showing the epicenter of the 2 May 2025 earthquake near Padang Panjang.

Table 1 Data Sources Used in This Study.

Data Type	Source
SAR Sentinel-1A SLC	https://scihub.copernicus.eu/
Administrative Map	https://tanahair.indonesia.go.id/portal-web/
DEM SRTM (30 m)	https://www.indonesia-geospasial.com/

The specific Sentinel-1A scenes used for the DInSAR analysis—covering pre- and post-earthquake acquisitions—are listed in Table 2.

Table 2. Sentinel-1A Image Data Used.

ID Scene	Date	Level	Orbit
S1A_IW_SLC__1SDV_20250408T114145_20250408T114212_058664_074388_E0A9	8 April 2025	1.0 (Single Look Complex)	Ascending
S1A_IW_SLC__1SDV_20250502T114145_20250502T114212_059014_0751C6_69F8	2 May 2025	1.0 (Single Look Complex)	Ascending
S1A_IW_SLC__1SDV_20250607T114144_20250607T114211_059539_07644F_BC5A	7 June 2025	1.0 (Single Look Complex)	Ascending

2.2 DInSAR Processing

The Differential Interferometric Synthetic Aperture Radar (DInSAR) technique was applied to quantify co-seismic ground deformation caused by the 2 May 2025 Padang Panjang earthquake. A structured interferometric workflow was implemented to separate deformation signals from topographic contributions and noise sources. The overall processing chain is illustrated in Figure 2.

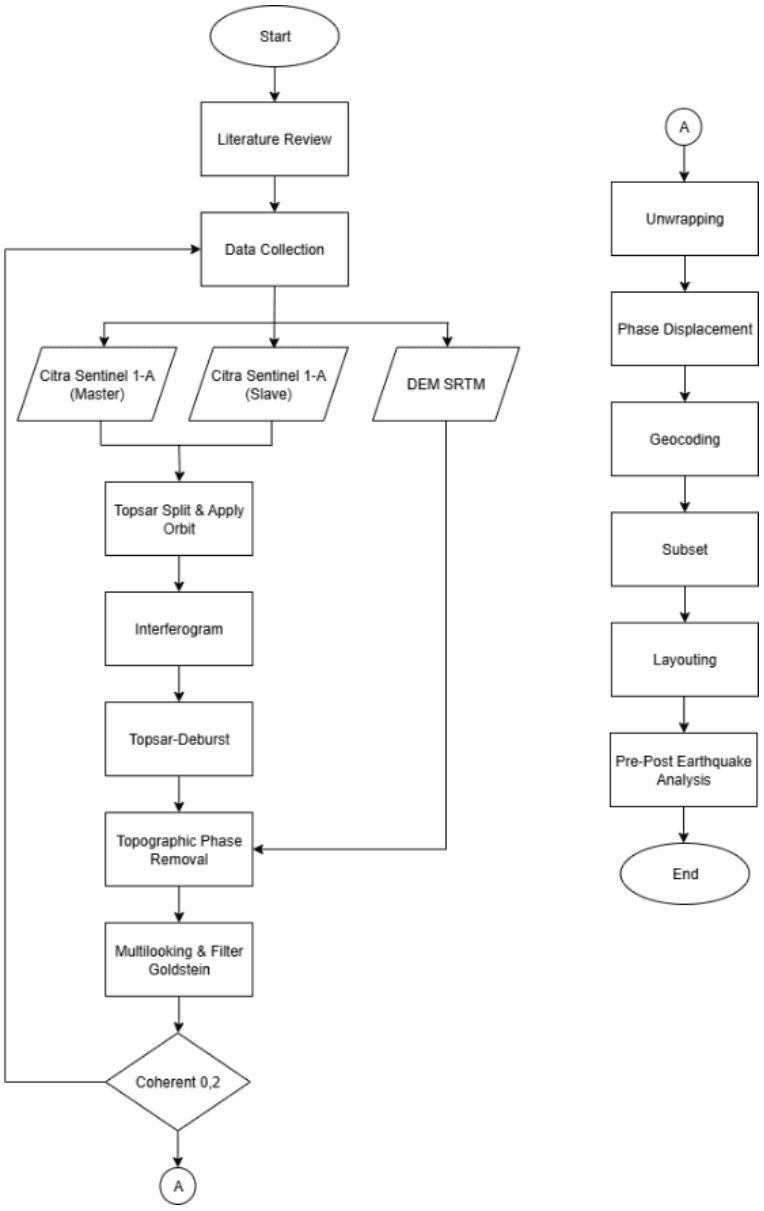

Figure 2. Workflow of DInSAR Processing.

2.2.1 Baseline Estimation and Coregistration Image

Baseline estimation was performed to evaluate the perpendicular baseline distance between SAR acquisitions, as shorter baselines generally preserve higher coherence. The selected image pairs satisfied baseline requirements suitable for deformation analysis. Coregistration was then conducted to align the master and slave images with sub-pixel accuracy. Accurate coregistration is critical because residual misalignment can introduce phase errors that degrade interferogram quality.

2.2.2 Interferogram Formation and Coherence Estimation

Interferograms were generated by calculating the phase difference between the coregistered SAR images. Coherence estimation was applied to assess the reliability of phase information at each pixel. In this study, a coherence threshold of 0.2 was applied. This threshold was selected as a compromise between retaining sufficient spatial coverage and excluding pixels dominated by noise, such as dense vegetation, water bodies, or areas affected by severe decorrelation. Coherence values below this threshold were masked to improve the robustness of the deformation interpretation.

2.2.3 Topographic Phase Removal

The interferometric phase contains contributions from surface deformation, topography, atmospheric delay, and orbital errors. To isolate the deformation component, the topographic phase was removed using the SRTM DEM with 30 m resolution. This step is essential to prevent elevation-related artifacts from being misinterpreted as ground displacement, particularly in areas with variable topography.

2.2.4 Filtering, Multilooking, and Subsetting

A Goldstein filter was applied to suppress high-frequency phase noise while preserving significant deformation fringes. Multilooking was then performed to reduce speckle noise and improve phase stability by spatial averaging. The dataset was subsequently subset to the Padang Panjang area to focus the analysis on the region affected by the earthquake and to optimize processing efficiency.

2.2.5 Phase Unwrapping and Deformation Conversion

Phase unwrapping is applied to convert the interferometric phase from a wrapped domain ($-\pi$ to $+\pi$) into a continuous value. After unwrapping, the phase is converted to displacement using the equation 1.

$$d = (\lambda \times \varphi) / (4\pi \times \cos(\theta)) \quad (1)$$

where d is the displacement, φ is the unwrapped phase (in radians), λ is the radar wavelength (5.6 cm for Sentinel-1A), and θ is the radar incidence angle. Note: the displacement values represent LOS (Line-of-Sight) movement, not pure vertical motion.

2.2.6 Data Analysis Technique

Deformation analysis was conducted by comparing interferograms from pre-earthquake and post-earthquake periods, each spanning approximately ±30 days from the event date. Fringe patterns were interpreted as indicators of surface displacement, where consistent and coherent fringes suggested ground movement related to seismic activity.

However, it is important to note that deformation signals at the millimeter scale are sensitive to atmospheric phase delays, particularly tropospheric effects. Residual atmospheric artifacts may persist despite short temporal baselines and coherence filtering, potentially influencing the magnitude and spatial distribution of the observed deformation. Therefore, the results were interpreted cautiously, emphasizing relative deformation patterns rather than absolute displacement values.

3. RESULTS AND DISCUSSION

3.1 Interferogram

The interferograms generated from the Sentinel-1A image pairs represent spatial variations in radar phase differences between two acquisition dates. These phase differences reflect changes in the

distance between the satellite sensor and the ground surface along the radar Line of Sight (LOS). Figure 3 presents the interferograms for the April–May 2025 and May–June 2025 periods, which serve as the initial qualitative representation of surface change prior to further processing.

At this stage, the interferograms mainly illustrate the spatial distribution of phase variations rather than definitive deformation. Therefore, interpretation is limited to identifying coherent patterns and areas suitable for subsequent analysis.

(a)

(b)

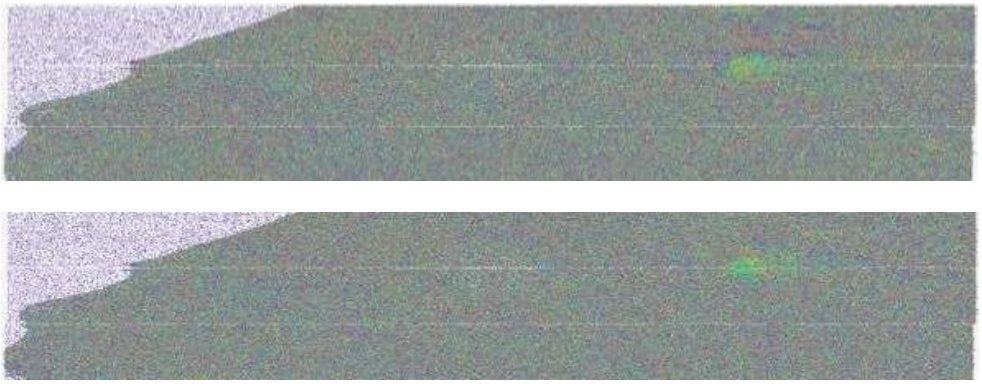

Figure 3. Interferogram results from (a) April–May 2025 and (b) May–June 2025**.**

3.2 TOPSAR Deburst

To improve spatial continuity, TOPSAR debursting was applied to remove burst boundaries inherent to Sentinel-1 TOPSAR acquisition. This process produced seamless interferograms by merging individual bursts into a single image. As shown in Figure 4, debursting reduced linear artifacts and enhanced visual continuity, supporting reliable interpretation in later stages.

(a)

(b)

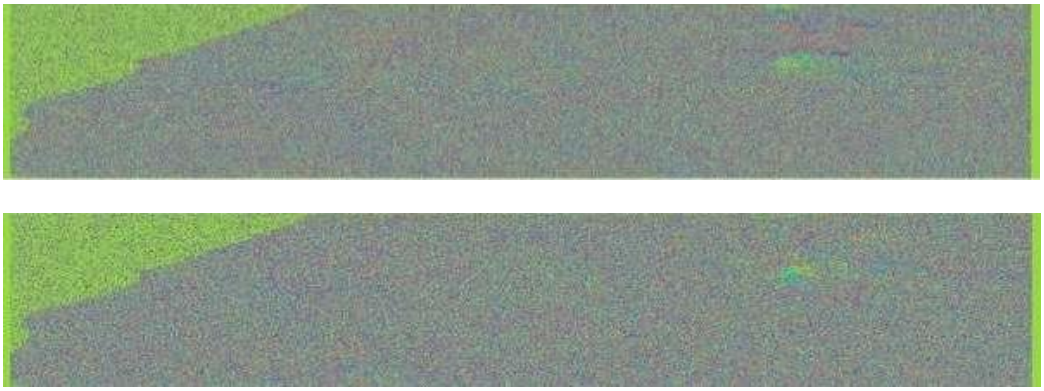

Figure 4. TOPSAR Deburst results on (a) April–May 2025 and (b) May–June 2025 imagery.

3.3 Filtered Interferogram Image

Filtering and multilooking were applied to suppress high-frequency noise and improve the signal-to-noise ratio. The filtered interferograms (Figure 5) exhibit clearer and more stable phase patterns compared to the unfiltered results. This step was particularly important given the small magnitude of expected deformation and the potential influence of atmospheric noise.

3.4 Phase Unwrapping

Phase unwrapping converted the wrapped phase values into a continuous phase surface, allowing spatial patterns to be examined more clearly. The unwrapped phase maps shown in Figure 6 reveal coherent phase variations across the study area for both time periods. At this stage, the results remain expressed in radians and do not yet represent physical displacement.

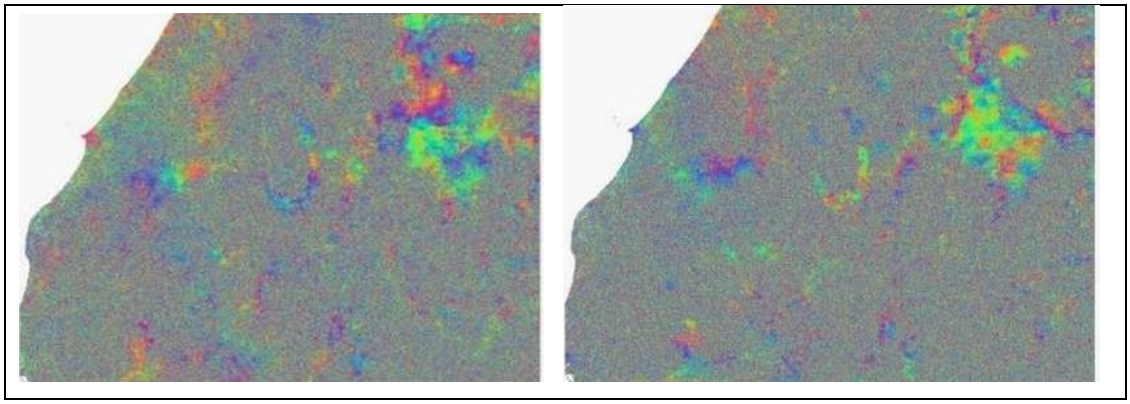

Figure 5. Interferogram after filtering and multilooking for (left) April–May 2025 and (right) May–June 2025 imagery.

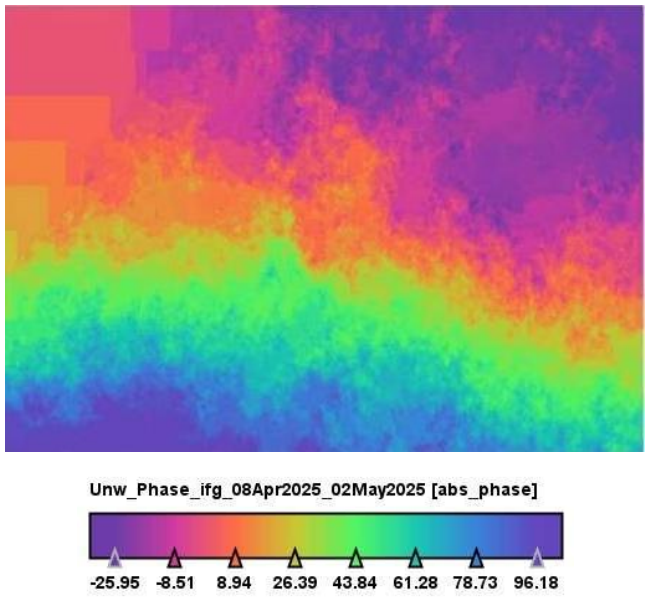

(a)

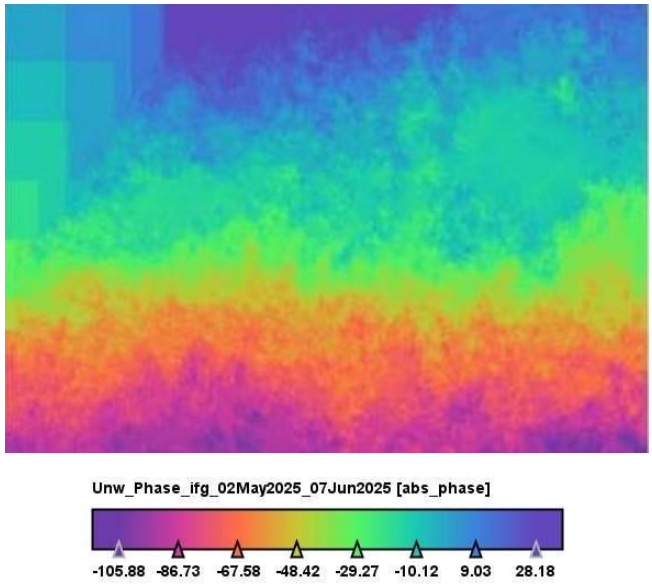

(b)

Figure 6. Unwrapped phase results for (a) April–May 2025 and (b) May–June 2025 imagery.

3.5 Phase-to-Displacement Conversion

The unwrapped phase was converted into displacement values using Equation (1), producing LOS displacement maps for each period (Figure 7). It is important to emphasize that these results represent displacement along the satellite LOS direction and do not correspond to pure vertical or horizontal ground motion.

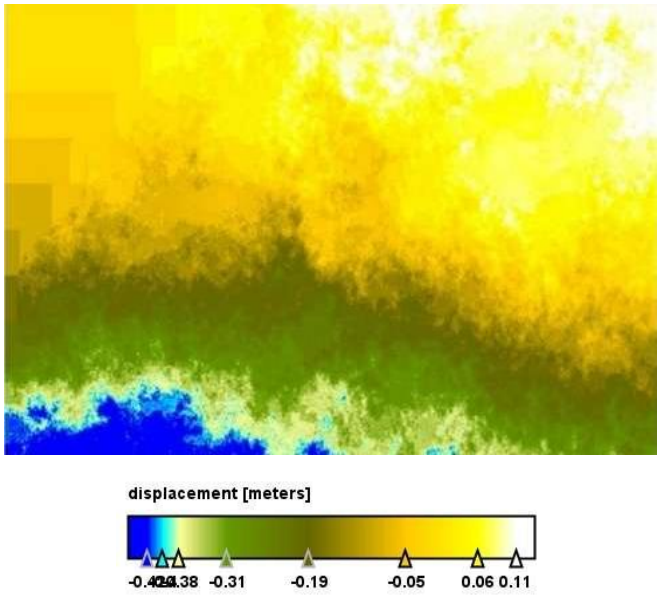

(a)

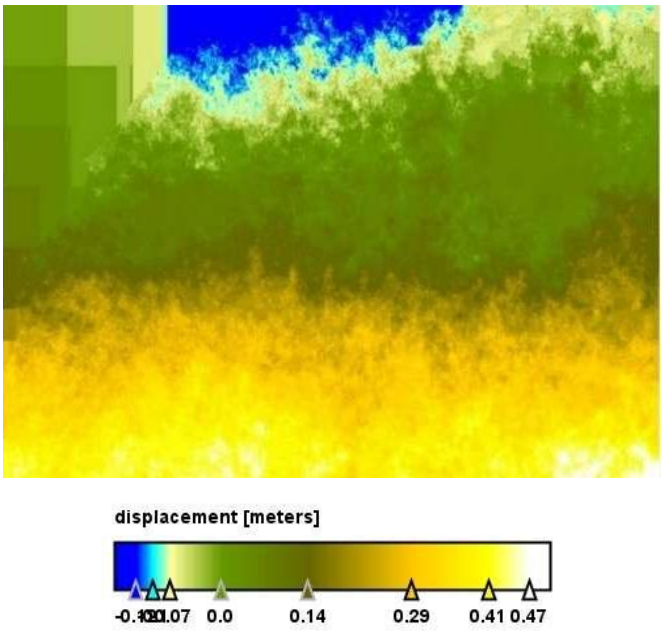

(b)

Figure 7. Displacement Results for (a) April–May 2025 and (b) May–June 2025.

3.6 Pre-Earthquake (8 April – 2 May 2025)

The LOS displacement map for the pre-earthquake period (Figure 8) shows relatively uniform values dominated by positive ranges between +0.0368 mm and +0.45 mm across most of the study area. These values are spatially widespread and do not exhibit localized concentration around known fault structures or the future epicentral zone.

Given the sub-millimeter magnitude of the observed values and their broad spatial distribution, these patterns are interpreted cautiously as background signals. They may reflect long-term surface trends, residual atmospheric delays, or interferometric noise rather than pre-seismic deformation. Therefore, no tectonic interpretation is attributed to the pre-earthquake displacement pattern.

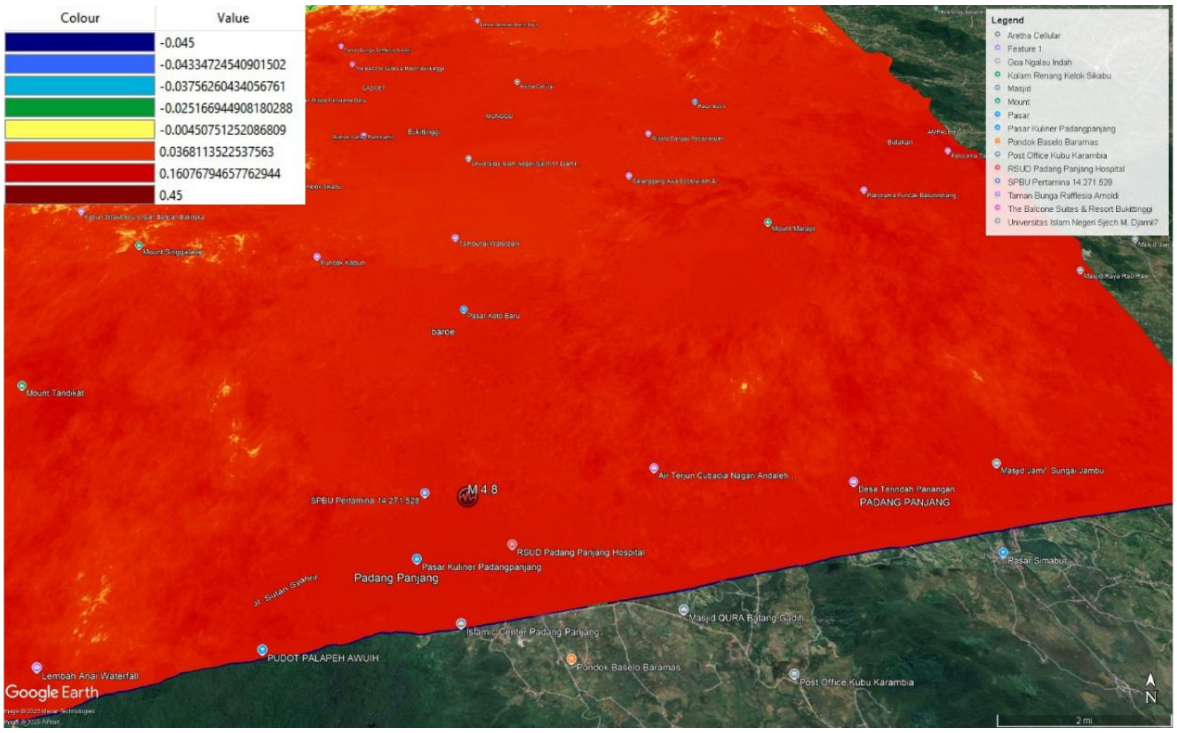

Figure 8. Pre-Earthquake (8 April – 2 May 2025).

3.7 Post-Earthquake (2 May – 7 June 2025)

The post-earthquake LOS displacement map (Figure 9) exhibits a more heterogeneous spatial pattern compared to the pre-event period. Negative LOS displacement values between −0.045 mm and −0.025 mm are concentrated in the central and southern parts of the study area, including the epicentral region and Padang Panjang City. Positive values are more prominent in the northern sector.

These results represent relative LOS displacement only. Without multi-geometry (ascending–descending) data or independent GNSS measurements, the observed patterns cannot be interpreted as vertical or horizontal ground motion. The spatial contrast, however, indicates a change in surface response following the earthquake.

3.8 Inter-Period Comparison

A comparison between the pre- and post-earthquake LOS displacement maps reveals a notable shift in displacement patterns near the epicentral area. The transition from predominantly positive LOS values in the pre-earthquake period to negative LOS values in the post-earthquake period suggests a relative change in surface response following the seismic event.

However, the magnitude of this difference, approximately on the order of sub-millimeter values, lies close to the sensitivity limits of C-band DInSAR. Atmospheric phase delays, residual decorrelation, and processing uncertainties may contribute to the observed differences. Therefore, the results are interpreted as indicative spatial patterns rather than definitive measurements of coseismic deformation.

Despite these limitations, the spatial consistency of the LOS displacement contrast highlights the potential of DInSAR to detect subtle surface responses associated with moderate-magnitude earthquakes. These findings should be considered as preliminary indicators that warrant further investigation using multi-orbit SAR data or ground-based validation.

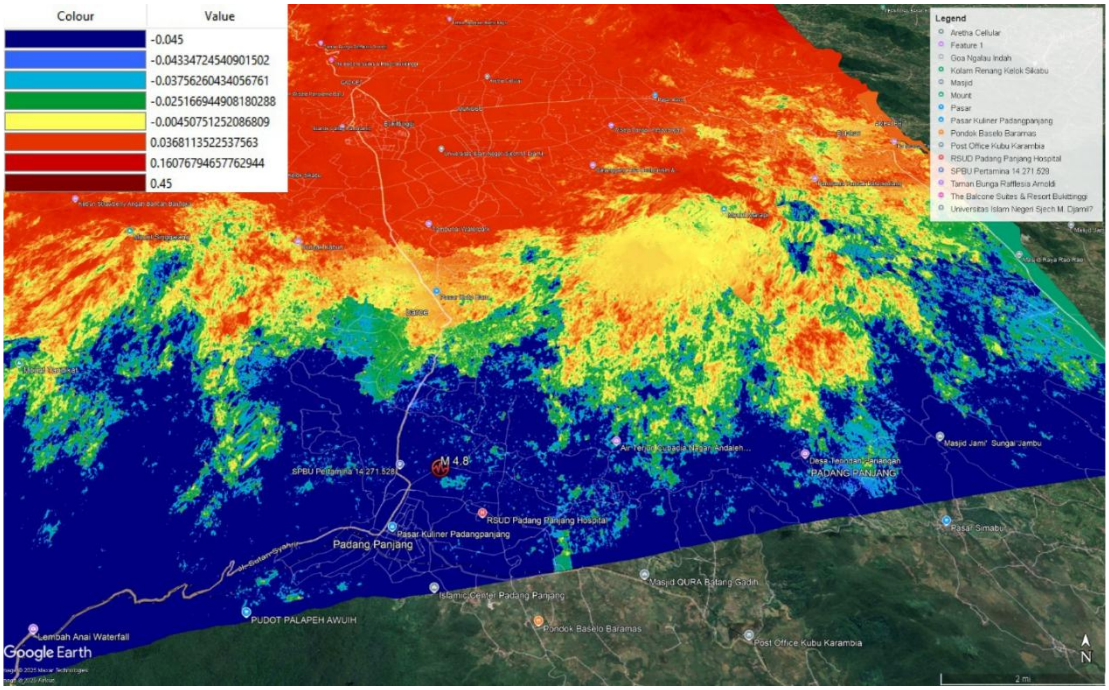

Figure 9. Post-Earthquake (2 May – 7 June 2025).

4. CONCLUSION

This study demonstrates the effectiveness of Differential Interferometric Synthetic Aperture Radar (DInSAR) as a methodological tool for detecting and visualizing subtle ground surface deformation associated with moderate seismic events. By applying DInSAR to the Padang Panjang region following the 2 May 2025 earthquake, the research successfully mapped localized vertical surface changes, with the most notable deformation concentrated near the epicentral area of the M 4.8 event. The detected cumulative vertical displacement of approximately −0.495 mm highlights the sensitivity of the method in capturing small-scale deformation that may not be easily observed through conventional ground-based measurements.

The primary objective of this research—to demonstrate the applicability of DInSAR for post-earthquake surface deformation analysis in an active tectonic setting—was achieved. Rather than providing a detailed quantitative interpretation of tectonic processes, the results emphasize the capability of the method to reveal spatial and temporal deformation patterns and their association with known geological structures, such as the Sianok Fault. The comparison between pre- and post-earthquake conditions illustrates how DInSAR can capture changes related to stress accumulation and release within the crust, thereby supporting its role as a monitoring and analytical approach.

The findings have important implications for seismic hazard assessment and geophysical monitoring, as DInSAR offers a cost-effective and wide-area technique for observing deformation in tectonically active regions like West Sumatra. However, this study is subject to limitations, including the relatively short temporal observation window, the small magnitude of the earthquake, and potential atmospheric and noise effects that may influence displacement accuracy. Future research should integrate longer time series data, higher-resolution SAR datasets, and complementary geodetic or geological information to strengthen interpretation and improve robustness. Overall, this research underscores the significance of DInSAR as a reliable methodological framework for surface deformation analysis and its potential contribution to earthquake-related studies and risk mitigation efforts.

ACKNOWLEDGEMENT

The author would like to express sincere gratitude to the Meteorology, Climatology, and Geophysics Agency (BMKG) for the opportunity to undertake an internship, which provided valuable

experience and insights that supported the completion of this research. The author also extends appreciation to the Department of Physics, Andalas University, for their guidance and support throughout this study.

REFERENCE

Azhari, M.F., Karyanto, K., Rasimeng, S., Mulyanto, B.S., 2020, Analisis deformasi permukaan menggunakan metode DInSAR (Differential Interferometry Synthetic Aperture Radar) pada studi kasus gempabumi Lombok periode Agustus 2018, *Jurnal Geofisika Eksplorasi*, Vol. 6, Hal. 131–144, https://doi.org/10.23960/jge.v6i2.68.

Fajriani, Q.R., Jayadi, R., Legono, D., 2019, Pengaruh intensitas hujan, jangkauan radar, dan topografi terhadap perkiraan hujan radar X-band multiparameter. In *Prosiding Seminar Nasional Pascasarjana Departemen Teknik Sipil FT-UI* (pp. 300–309). Yogyakarta, Indonesia.

Hanssen, R. F. (2001). *Radar interferometry: Data interpretation and error analysis*. Dordrecht: Kluwer Academic Publishers

Jensen, J.R., 2015, *Introductory digital image processing: A remote sensing perspective* (4th ed.). Upper Saddle River, NJ: Prentice Hall.

Massonnet, D., & Feigl, K. L. (1998). Radar interferometry and its application to changes in the Earth's surface. *Reviews of Geophysics, 36*(4), 441–500. https://doi.org/10.1029/97RG03139

Oktaviani, S., Sari, D.K., 2024, Analisis deformasi permukaan pada bencana gempa bumi menggunakan metode Differential Interferometric Synthetic Aperture Radar (DInSAR). *Prosiding Seminar Nasional*, 582–587.

Palano, M., 2023, Ground deformation patterns detection by InSAR and GNSS techniques. *Remote Sensing, 15*, 1–4, DOI: 10.3390/books978-3-0365-6887-4.

Pepe, A., 2012, Advanced multitemporal phase unwrapping techniques for DInSAR analyses. In I. Padron (Ed.), *Synthetic aperture radar* (pp. 57–82). Rijeka, Croatia: InTech.

Pepe, A., Calò, F., 2017, A review of interferometric synthetic aperture radar (InSAR) multi-track approaches for the retrieval of Earth's surface displacements. *Applied Sciences, 7*(12), 1264. https://doi.org/10.3390/app7121264.

Pusat Litbang Perumahan dan Permukiman Kementerian PUPR. (2017). *Peta gempa Indonesia 2017*. Jakarta: Kementerian PUPR.

Rafie, M.T., Sahara, D.P., Cummins, P.R., Triyoso, W., Widiyantoro, S., 2023, Stress accumulation and earthquake activity on the Great Sumatran Fault, Indonesia. *Natural Hazards, 116*, 3401–3425. https://doi.org/10.1007/s11069-023-05816-2.

Raharjo, F.D., Syafriani, Sabarani, A.Z., 2016, Analisis variasi spasial parameter seismotektonik daerah Sumatera Barat dan sekitarnya dengan menggunakan metode likelihood. *Pillar of Physics, 8*, 73–80.

Raimadoya, M.A., Trisasongko, B.H., Shiddiq, D., Panuju, D.R., Maulida, R., 2004, Pengolahan DSM dengan interferometri SAR (InSAR) antariksa untuk mekanisme pembangunan bersih (MPB) Protokol Kyoto. *Jurnal Ilmu Tanah dan Lingkungan, 6*(2), 39–45. https://doi.org/10.29244/jitl.6.2.39-45.

Sari, L.D., 2025, Padang Panjang digoyang gempa, guncangannya mengagetkan warga. *METROTV*.

Turcotte, D.L., Gerald, S., 2014, Stress and strain in solids. In *Geodynamics* (pp. 73–104). Cambridge: Cambridge University Press.